Electronic supplementary information for

Stabilizing benzene-like planar N_6 rings to form a single atomic honeycomb BeN_3 sheet with high carrier mobility

Xiaoyin Li,[a,b] Shunhong Zhang,[c] Cunzhi Zhang,[b] and Qian Wang*[a,b]

[a]Center for Applied Physics and Technology, College of Engineering, Peking University; Key Laboratory of High Energy Density Physics Simulation, Ministry of Education, Beijing 100871, China

[b]Department of Materials Science and Engineering, College of Engineering, Peking University, Beijing 100871, China

[c]Institute for Advanced Study, Tsinghua University, Beijing 100084, China

1. Other low-energy structures of BeN_3

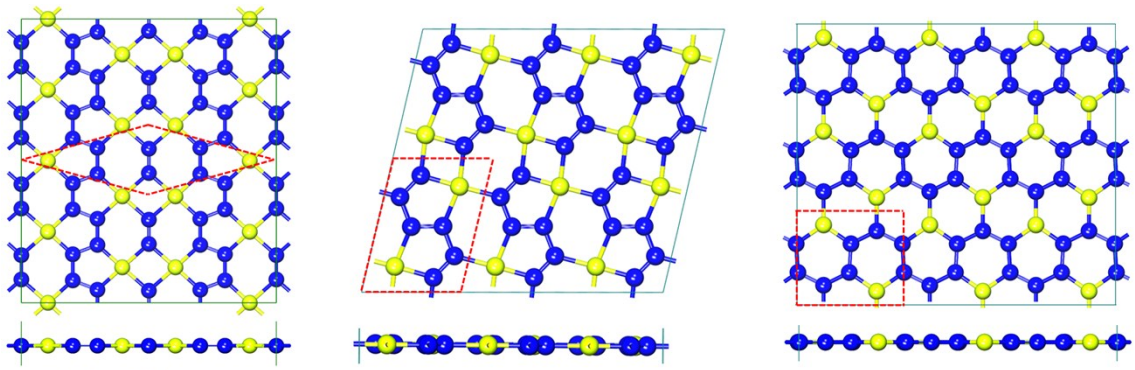

Fig. S1 Structures of other low-energy isomers of BeN_3 found by using the global structure search method and the comparison of their relative energies with respect to that of the lowest-energy structure *h*-BeN_3. The red dashed lines denote unit cells.

2. IR and Raman spectra of *h*-BeN_3

With D_{6h} point symmetry, the optical modes of *h*-BeN_3 at the Γ point can be represented as ("I" and "R" represent the infrared and Raman activity respectively)

$$\Gamma_{optical}\,(h\text{-}BeN_3) = A_{1g}\,(R) \oplus A_{2g} \oplus 2A_{2u}\,(I) \oplus B_{1g} \oplus B_{1u} \oplus B_{2u} \oplus 2E_{1u}\,(I) \oplus E_{2u} \oplus E_{1g}\,(R) \oplus 3E_{2g}\,(R). \quad (1)$$

Those modes with A_{1g}, E_{1g}, or E_{2g} symmetry have Raman activity, while those modes with A_{2u} or E_{1u} symmetry have IR activity.

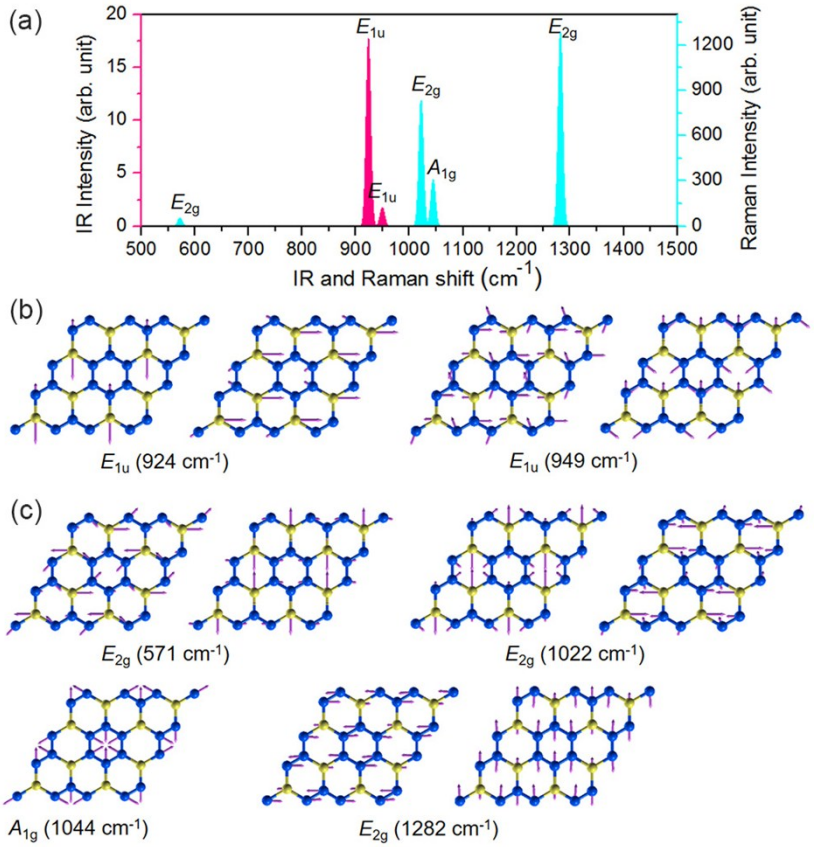

Fig. S2 (a) IR and Raman spectra of *h*-BeN_3 (arb. unit represents arbitrary unit). (b) and (c) are the vibration modes corresponding to the peaks in IR and Raman spectra, respectively.

3. Thermal stability of *h*-BeN_3

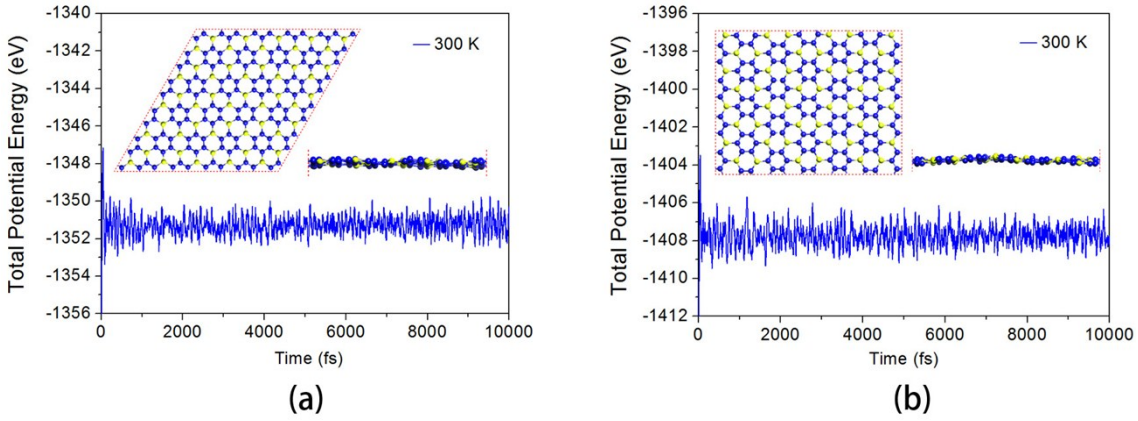

Fig. S3 Fluctuation of the total potential energy during AIMD simulations at temperature of 300 K with supercell of (a) (5×5) and (b) (3√3×4) respectively. Insets are snapshots of the structures at the end of the simulations.

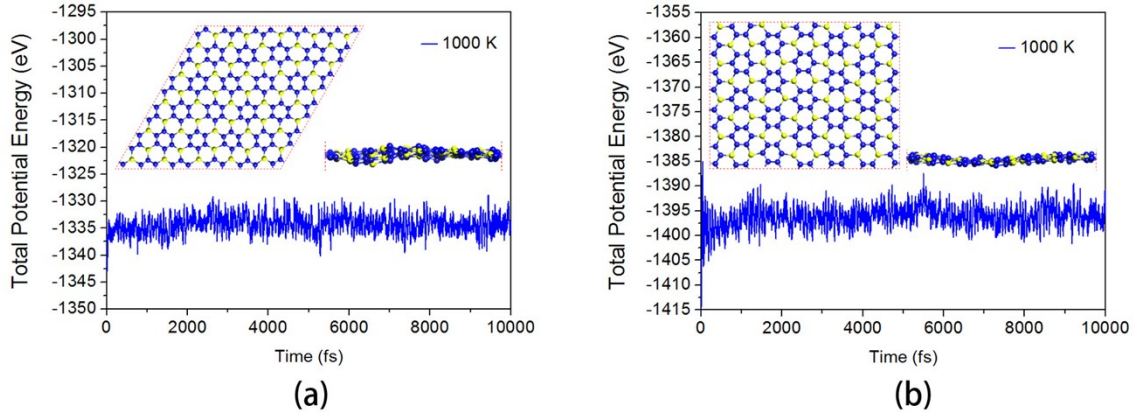

Fig. S4 Fluctuation of the total potential energy during AIMD simulation at temperature of 1000 K with supercell of (a) (5×5) and (b) (3√3×4) respectively. Insets are snapshots of the structures at the end of the simulations.

4. Tight-binding model of *h*-BeN_3

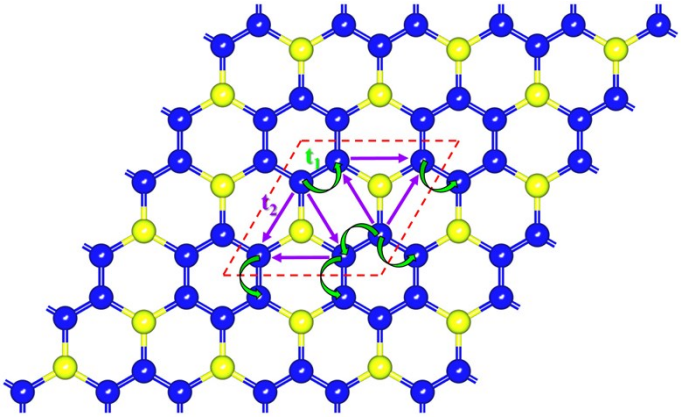

Fig. S5 Illustration of intra-ring hopping (green arrows, t_1) and inter-ring hopping (purple arrows, t_2) between N-p_z orbitals. The red rhombus denotes the unit cell of *h*-BeN_3.

5. Carrier mobility of *h*-BeN_3

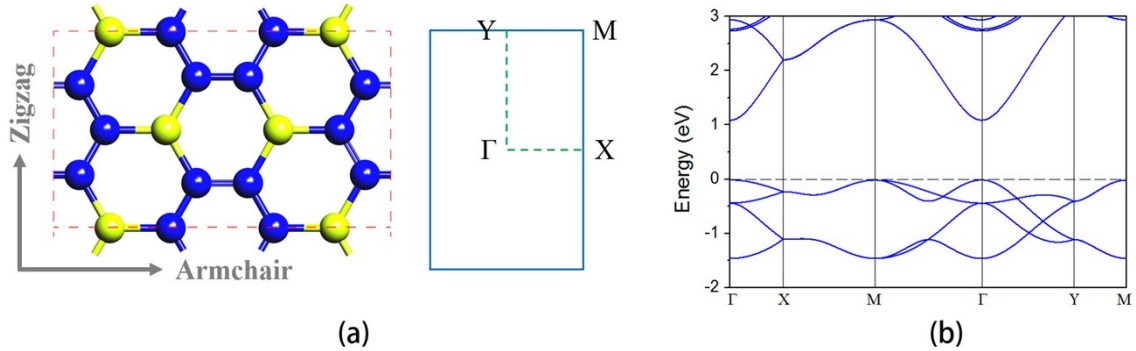

Fig. S6 (a) Atomic structure of *h*-BeN_3 in an orthogonal supercell and its corresponding Brillouin zone. (b) Electronic band structure of *h*-BeN_3 in the orthogonal lattice. Note that due to Brillouin zone folding, both Γ and M points become VBM, but we only consider the hole effective mass at Γ.

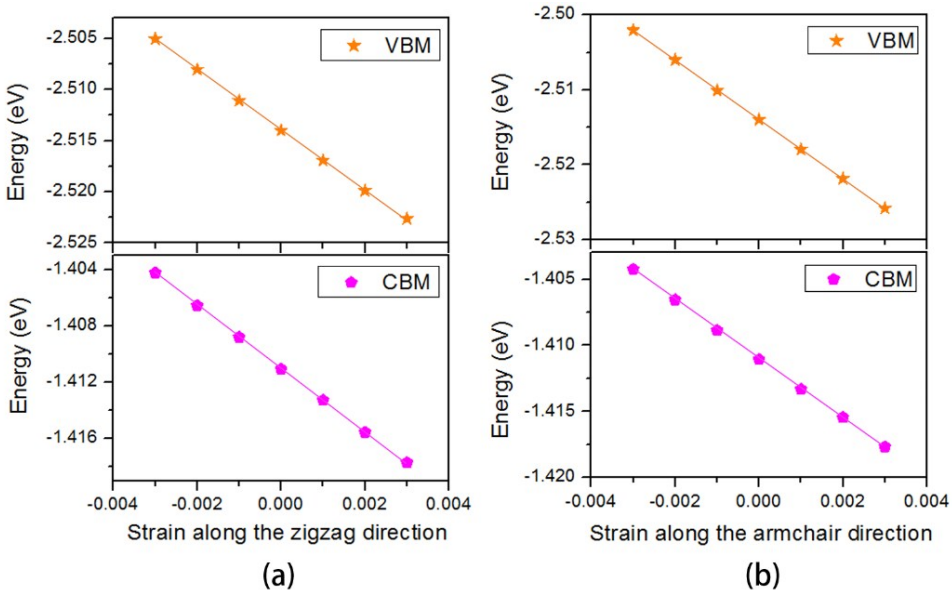

Fig. S7 Energy shift of the band edge (VBM and CBM) with respect to the lattice dilation and compression along the (a) zigzag and (b) armchair directions, respectively.